

Electronic Supplementary Information for

**Synergetic Role of Charge Transfer and Strain
Engineering in Improving the Catalysis of Pd Single-
Atomic-thick motifs Stabilized on Defect-free
MoS₂/Ag(Au)(111) Heterostructure**

Zhixin Su,^a Rui pang,^a Xiaoyan Ren,^{*a} and Shunfang Li^{*a}

*^aSchool of Physics and Microelectronics, Zhengzhou University, Zhengzhou, Henan
450001, China.*

This file includes:

Table S1 Work function of the typical systems.

Table S2 Calculated O-O bond lengths, O₂-CO distances (d in Å) in the key steps for CO oxidations via TER mechanism.

Table S3 Adsorption energies of CO, O₂, 2CO, and O₂+CO on only one Pd active site

Fig. S1 (a) Geometric structures and average cohesive energies (ACE) of the most stable structures of Pd_N clusters, (b) The second order difference of the ACE

Fig. S2 Average adsorption energy (E_a) of the most stable structural configurations of 3D-Pd_N species (N=4-7) with different configurations and adsorption sites.

Fig. S3 Average adsorption energy (E_a) of the most stable structural configurations of 2D-Pd_N species (N=3-7) with different configurations and adsorption sites.

Fig. S4 Energy barrier for the phase transition from the 2D to 3D configurations.

Fig. S5 Electronic density of states (DOS) of CO adsorbed on (a) Pd₁/MoS₂, (b) Pd₁/MoS₂/5.18%, (c) Pd₁/MoS₂/Au(111), and (d) Pd₁/MoS₂/Ag(111).

Fig. S6 Schematic show TER mechanism of the CO oxidation on Pd₁/substrates.

Fig. S7 Charge transfer (ΔQ) analysis of the CO oxidation (CLH) processes on 2D-Pd₃ species deposited on MoS₂, MoS₂/5.18%, MoS₂/Au(111), and MoS₂/Ag(111) substrates.

Table S1 Calculated work function (WF in eV) of the typical systems.

	MoS ₂	Au(111)	Ag(111)	MoS ₂ / Au(111)	MoS ₂ / Ag(111)	Pd ₁ /MoS ₂ / Au(111)	Pd ₁ /MoS ₂ / Ag(111)
WF	5.68	5.18	4.61	5.36	4.76	4.96	4.67

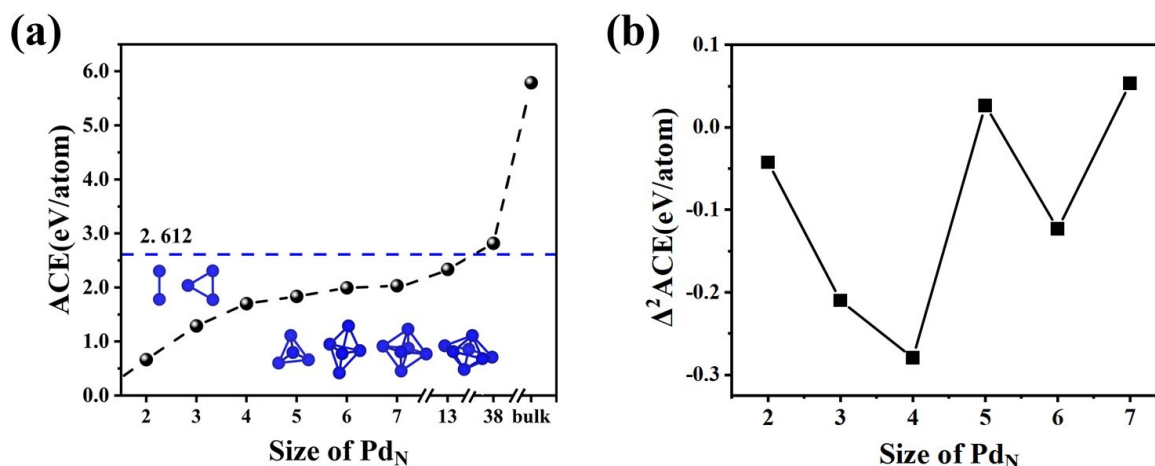


Fig. S1 (a) Geometric structures and average cohesive energies (ACE) of the most stable structures of Pd_N clusters ($N = 2-7$) in gas phase. (b) The second order difference of the ACE presented in (a).

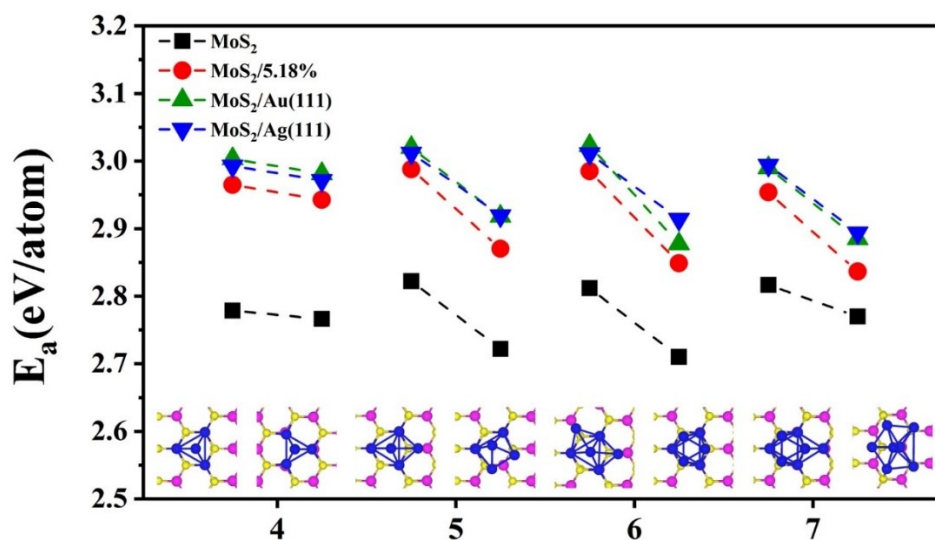


Fig. S2 Average adsorption energy (E_a) of the most stable structural configurations of 3D-Pd_N species ($N=4-7$) with different configurations and adsorption sites.

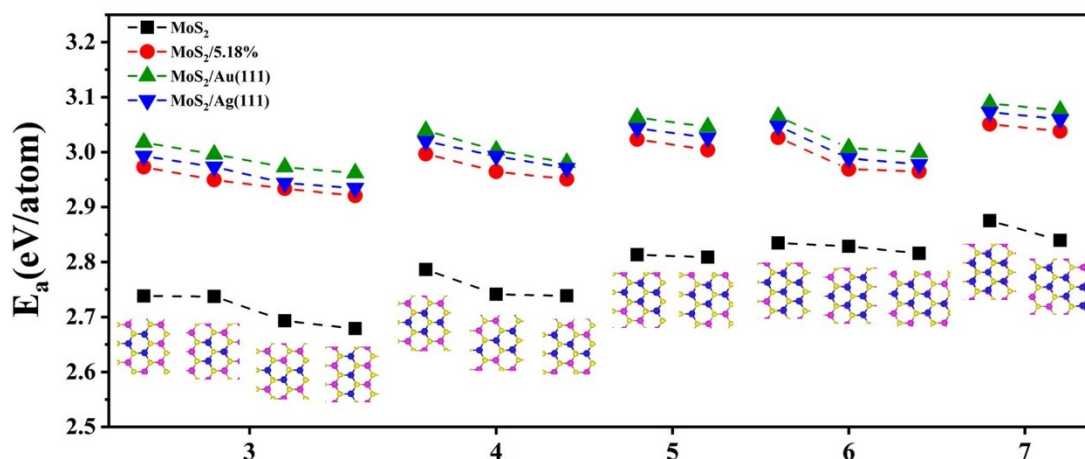


Fig. S3 Average adsorption energy (E_a) of the most stable structural configurations of 2D-Pd_N species ($N=3-7$) with different configurations and adsorption sites.

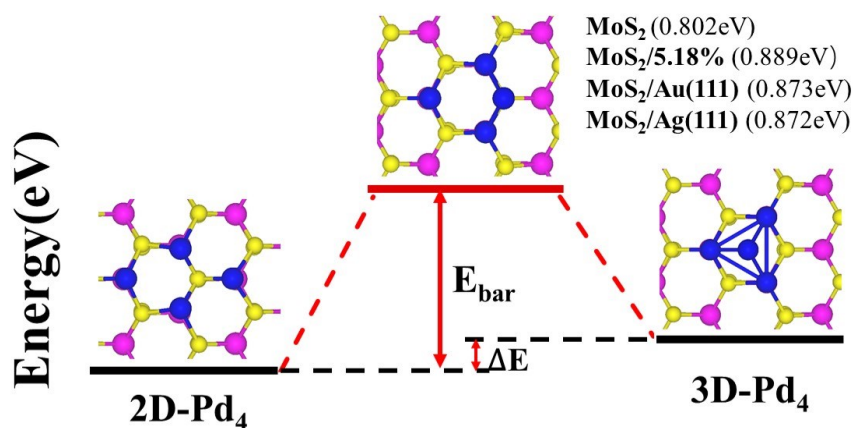


Fig. S4 Energy barrier (E_{bar}) for the phase transition from the 2D to 3D configurations.

we have demonstrated that, it is 2D-Pd₃ (rather than 2D-Pd₄) which displays significantly magic properties in the stability. Therefore, in experiment, 2D-Pd₃

possesses much longer life time than that of both 2D(3D)-Pd₄ and Pd₅. Moreover, as seen from **Fig. S4** even for the less stable species Pd₄, the calculated energy barrier (E_{bar}) for the phase transition from the 2D to 3D configurations is $E_{\text{bar}}=0.872$ eV, which is significantly higher than the CO oxidation reaction barrier of 0.410 eV. According to the Arrhenius form of $R=R_0 \times \exp[-E_{\text{bar}}/(k_{\text{B}}T)]$, with a typical prefactor of $R_0=10^{12}/\text{s}$, yielding a 2D to 3D phase transition rate of $2.253 \times 10^{-3}/\text{s}$ at $T \sim 300\text{K}$; nevertheless, the calculated $E_{\text{bar}}=0.763$ eV leads to a reaction rate of $1.526 \times 10^{-1}/\text{s}$ at $T \sim 300$ K for the phase transition from the 3D to 2D, which is about two orders of magnitude larger than that of the reversed process. These data suggest that, even though some 3D-Pd_N cluster may coexist with the 2D-Pd_N configurations, the 2D-Pd_N motifs should be dominant in experimental observations.

Table S2 Calculated O-O bond lengths, O₂-CO distances (d in Å) in the key steps shown in **Fig. 5(a)** for CO oxidations via TER mechanism on Pd₃/MoS₂, Pd₃/MoS₂/5.18%, Pd₃/MoS₂/Au(111), and Pd₃/MoS₂/Ag(111).

d(Å)	CO-O ₂ (IS)	O-O (IS)	CO-O ₂ (TS1)	O-O (TS1)	CO-O ₂ (PS)	O-O (PS)	O-O (TS2)
MoS ₂	3.325	1.273	1.843	1.315	1.336	1.434	1.434
MoS ₂ /5.18%	3.251	1.277	1.748	1.332	1.328	1.440	1.772
MoS ₂ /Au(111)	3.321	1.275	1.746	1.330	1.329	1.440	1.774
MoS ₂ /Ag(111)	3.255	1.283	1.696	1.347	1.357	1.437	1.762

Table S3 Adsorption energies (E_a in eV) of one CO, O₂, two CO (2CO), and O₂ and CO (O₂+CO) on only one Pd active site.

E_a (eV)	CO	O ₂	2CO	O ₂ +CO
MoS ₂	1.372	0.586	2.588	1.667
MoS ₂ /5.18%	1.106	0.562	2.290	1.385
MoS ₂ /Au(111)	1.107	0.568	2.324	1.135
MoS ₂ /Ag(111)	1.115	0.651	2.320	1.135

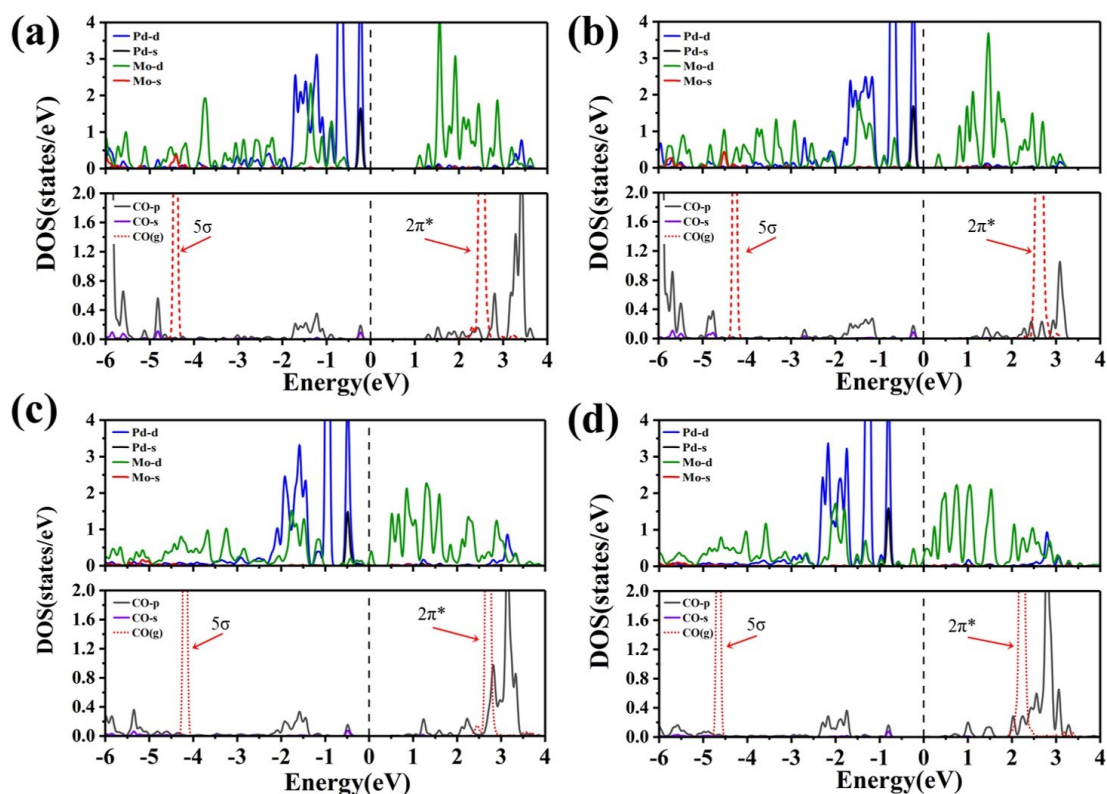


Fig. S5 Electronic density of states (DOS) of CO adsorbed on (a) Pd₁/MoS₂, (b) Pd₁/MoS₂/5.18%, (c) Pd₁/MoS₂/Au(111), and (d) Pd₁/MoS₂/Ag(111). For comparison, the DOS of gas phase CO far (more than 5 Å) above the Pd₁/substrates are also presented in red and dashed lines, with the Fermi levels shifted to zero.

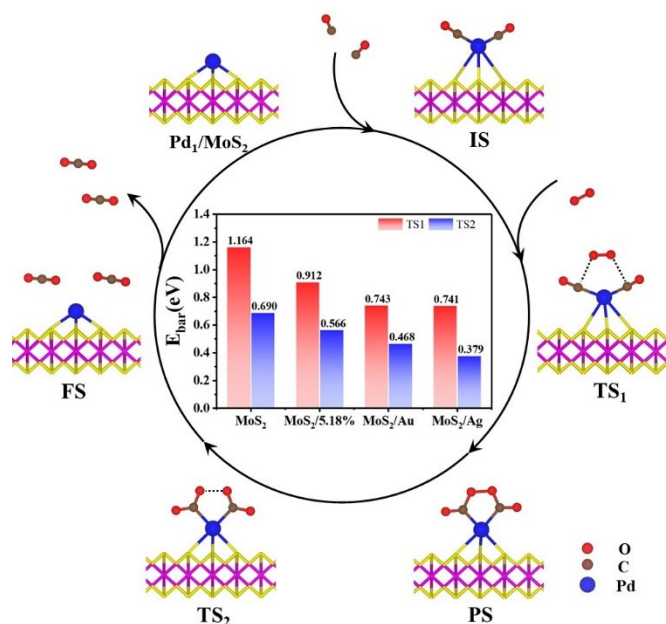


Fig. S6 Schematic show of the CO oxidation on Pd₁/substrates. TER mechanism, with the E_{bar} obtained in TS₁ and TS₂.

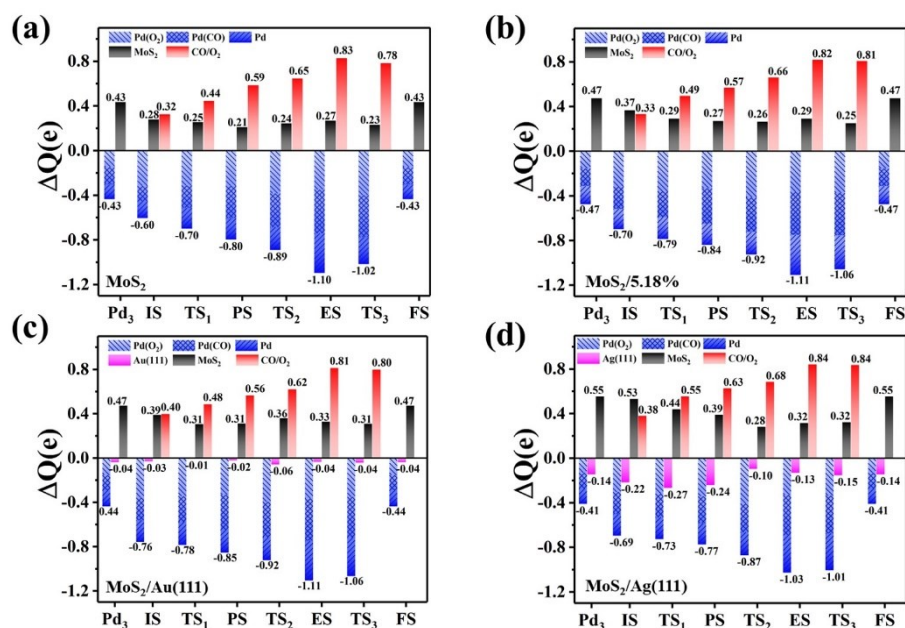


Fig. S7 Charge transfer (ΔQ) analysis of the CO oxidation (CLH) processes on 2D-Pd₃ species deposited on MoS₂, MoS₂/5.18%, MoS₂/Au(111), and MoS₂/Ag(111) substrates. Here, the three Pd atoms in 2D-Pd₃ magic motifs are tabbed as Pd(O₂), Pd(CO), and Pd, on which O₂, CO, and no molecule is adsorbed, respectively.